Hydrol. Earth Syst. Sci. Discuss., https://doi.org/10.5194/hess-2017-647
Manuscript under review for journal Hydrol. Earth Syst. Sci.
Discussion started: 21 November 2017
© Author(s) 2017. CC BY 4.0 License.

Hydrology and Earth System Sciences
Discussions

Groundwater origin, flow regime and geochemical evolution in arid endorheic watersheds: a case study from the Qaidam Basin, Northwest China

Yong Xiao[1,2], Jingli Shao[1*], Shaun K. Frape[2], Yali Cui[1], Xueya Dang[3], Shengbin Wang[4], Yonghong Ji[5]

[1]School of Water Resources and Environment, China University of Geosciences (Beijing), Beijing, 100083, China
[2]Department of Earth and Environmental Sciences, University of Waterloo, Waterloo, N2L 3G1, Canada
[3]Xi'an Center of Geological Survey, China Geological Survey, Xi'an, 710054, China
[4]Bureau of Qinghai Environmental Geological Prospecting, Xining, 810007, China
[5]Lunan Geo-Engineering Exploration Institute of Shandong Province, Yanzhou, 272100, China

Correspondence to: Jingli Shao (jshao@cugb.edu.cn)

Abstract. Groundwater origin, flow and geochemical evolution in the Golmud River watershed of the Qaidam Basin was assessed using hydrogeochemical, isotopic and numerical approaches. Results show groundwater in the basin originates from precipitation and melt water in the mountainous areas of the Tibetan Plateau. Modern water was found in the alluvial fan and shallow aquifers of the loess plain. Deep confined groundwater was recharged by paleo-water during the late Pleistocene and Holocene under a cold climate. Groundwater in the low-lying depression of the central basin is composed of paleo-brines migrated from the western part of the basin due to tectonic uplift in the geological past. Groundwater chemistry is controlled by water-rock interaction and evaporation-salt precipitation, and varies from fresh to brine with the water types evolving from HCO_3·Cl-Ca·Mg·Na to Cl-Na, Cl-K-Na and Cl-Mg type waters along the flow path. The groundwater flow pattern is closely related to stratigraphic control and lithological distribution. Three hierarchical groundwater flow systems, namely local, intermediate and regional, were identified using numerical modelling. The quantity of water discharge from these three systems accounts for 82.69%, 14.26% and 3.05%, respectively, of the total groundwater quantity of the watershed. This study can enhance the understanding of groundwater origin, circulation and evolution in the Qaidam Basin as well as other arid endorheic watersheds in northwest China and elsewhere worldwide.

Keywords. Groundwater origin; Hydrogeochemistry; Groundwater flow pattern; Arid area; Qaidam Basin

1 Introduction

Closed basins in arid and semiarid areas have been the focus of attention due to their water scarcity, fragile ecology and rich mineral resources related to salt lakes (Edmunds et al., 2006; Lowenstein and Risacher, 2009; He et al., 2015; Herrera et al., 2016). Groundwater plays a vital role in water supply, ecology maintenance, transportation of chemical components, as well as the formation of oil, gas reservoirs and mineral resources in these basins (Toth, 1980; Jiang et al., 2014; Jiao et al., 2015;

© Author(s) 2017. CC BY 4.0 License.

Xiao et al., 2017). Understanding the regimes of groundwater recharge, flow and hydrogeochemical evolution are essential to maintain proper management, and implement sustainable utilization of groundwater and mineral resources, as well as maintaining the ecological environment (Herrera et al., 2016).

In the arid northwest of China there are many closed basins such as the Tarim, Qaidam, Junggar, and Minqin Basin, in which the low-lying discharge areas are occupied by saline lakes, salt playas and salt crusts. The Qaidam Basin (Fig.1a, b), the largest closed basin of the Tibetan Plateau, has the most plentiful number of salt lakes and salt playas and almost all varieties of salt deposits (Zheng et al., 1993), as well as rich oil and gas reservoirs (Tan et al., 2011; Ye et al., 2014). Considerable research has been conducted to provide support for water supply and mineral resource exploitation in the basin (Chen and Bowler, 1986; Vengosh et al., 1995; Lowenstein and Risacher, 2009; Li et al., 2010; Tan et al., 2011; Hou et al., 2014; Ye et al., 2014; Chen et al., 2017). However, most of the previous studies focused on the groundwater in the piedmont areas (Wang and Ren, 1996; Wang et al., 2010; Zhang, 2013; Hou et al., 2014; Su et al., 2015; Xu et al., 2017), material source of salt lakes (Vengosh et al., 1995; Lowenstein and Risacher, 2009; Tan et al., 2011; Chen et al., 2015), and the evolution of salt lakes (Chen and Bowler, 1986; Chen et al., 2017). Although several studies were performed to reveal the regional groundwater regimes (Tan et al., 2009; Gu et al., 2017; Xiao et al., 2017), very little research reported the circulation and evolution of groundwater from the mountain pass areas to the central terminal lake area due to the notable difficulties to move through and access the swamps on the lacustrine plain. This would greatly limit the understanding of the role of hydrogeological processes in the basin.

Hydrogeological survey efforts were undertaken in the Golmud River watershed of the basin since 2015, and developed a better understanding of regional hydrogeological conditions. The main objective of this study is to assess the regional hydrogeological regime of closed basins in the arid northwest of China, using the Golmud River watershed as a case study. To achieve this aim, a comprehensive approach using isotopes and hydrochemistry coupled with numerical simulation was performed. Environmental isotopes can provide valuable information on the origin, recharge environment and residence time of groundwater (Awaleh et al., 2017; Huang et al., 2017; Xiao et al., 2017). Hydrochemical composition has recorded the recharge water characteristics, hydrostratigraphic information, geochemical interaction, and other processes along the groundwater flow path (Redwan and Moneim, 2015; Verma et al., 2016), and thus can be used to track groundwater evolution. Numerical simulation of groundwater flow is an essential tool to synthesize hydrogeological information and reveal groundwater flow patterns (Bredehoeft and Konikow, 2012; Anderson et al., 2015; Tóth et al., 2016).

2 Study area

The Qaidam Basin is a large closed basin located on the north-eastern margin of the Tibetan plateau, and surrounded by the Qilian Mountains to the north, the Kunlun Mountains to the south, and the Altun Mountains to the west (Fig.1b). The study area, Golmud River Watershed (GRW), is located in the southern part of the Qaidam Basin with the second largest river, the Golmud River, running from the Kunlun Mountains in the south to the low-lying depression in the north central part of the

© Author(s) 2017. CC BY 4.0 License.

Basin (Fig.1c). The Qarhan salt lake is the largest salt lake in China at the northern margin of the GRW, adjacent to the Golmud River's Terminal Lake Dabusun. The third largest city on the Tibetan plateau, Golmud City, is also located in the GRW.

The out cropping stratigraphy of the GRW range from Proterozoic to Quaternary. The Quaternary strata are found in the mountainous area to the south. These strata have undergone magmatic activity, uplift, tectonic movements, as well as intense weathering, resulting in massive material sources of sediments to the basin. The Quaternary deposits have thicknesses ranging from hundreds of meters in the piedmont area to thousands of meters in the low-lying depression (basin center) (Zheng et al., 1993; Chen et al., 2017). The regional Quaternary aquifers in the basin vary from single unconfined gravel and sand layers in the alluvial fan to multi-layers of silt and clay in the low-lying depression (basin center). Three continuous aquitards (clay layers) are found in the basin at depths of 60 m, 290 m and 450 m, respectively (Fig.8), which have had a significant influence on confining groundwater flow.

Salt crusts are formed on the ground surface in locations near the terminal areas of streams. Core drilling records also show many salt-bearing deposits are observed throughout the strata (Chen and Bowler, 1986). Based on the terrain, sediments and hydrogeological condition, the study area can be divided into 5 zones. Zone 1 is the Kunlun mountainous area, and Zone 2 is the alluvial fan plain at the Kunlun piedmont. Zone 3, 4 and 5 belong to the loess plain, and Zone 3 is the main groundwater overflow (discharge) zone of the watershed, and Zone 5 is the terminal lake zone (low-lying depression of the watershed) with the salt crust and playa, Zone 4 is the transition zone (middle-lower stream area of the watershed) between Zone 3 and 5. The climate in the GRW is extremely variable, both spatially and temporally. Precipitation in the Kunlun Mountains is more than 200 mm per year, but less than 50 mm in the basin, and also presents a gradual decreasing trend from the piedmont area to the low-lying central depression. The potential evaporation is extremely high (＞2600 mm per year). This hyper-arid climate results in aquifers in the basin that do not obtain effective recharge from the local precipitation. Overall, groundwater in the basin originates from Golmud River seepage and bedrock lateral flow in the alluvial fan, and topography results in flow towards the low-lying depression (basin center).

3 Materials and Methods

3.1 Hydrochemical and isotopic sampling and analytical methods

A total of 228 water samples were collected from GRW in 2015 and 2016, including 180 groundwater samples and 48 surface water samples (42 river water and 6 lake water samples) (Fig.1c). Groundwater samples were collected from both shallow phreatic aquifers and deep confined aquifers. Surface water samples were obtained along the Golmud River, as well as from Lake Qarhan, Lake Dabusun and other small lake in the low-lying depression area (basin center). In addition, one snow (snowmelt water) sample, 8 precipitation samples and 90 brine water samples (groundwater) with hydrogen and oxygen stable isotope data were obtained from China's stable isotope geochemistry database (http://210.73.59.163/isogeochem/). The location of the snow and precipitation samples are shown on Fig.1c. The detailed

© Author(s) 2017. CC BY 4.0 License.

locations of 90 brine water samples are not known, but it is known that all of these samples were collected from the Qarhan salt playa and Bieletan salt playa (Fig.1c).

For groundwater sampling, all wells and boreholes, except those that were artesian, were pumped for several well volumes to remove the stagnant water in the wells and boreholes, and monitored until the electrical conductivity (EC) of the pumping water was stable. The sampling procedure followed is described in Huang et al. (2016) and Chen et al. (2011). Samples for major element analysis were collected in two 250 ml high density polyethylene bottles after filtration using 0.45 μm filter membranes (Huang et al., 2016). Samples for tritium (^{3}H) and stable isotopes (^{2}H, ^{18}O) analysis were collected in 500 ml and 50 ml glass bottles, respectively, that were filled to overflowing after rinsing and were sealed tightly. ^{14}C samples were collected by adding $BaCl_2$ and CO_2-free NaOH to 120 L groundwater at pH=12, obtaining $BaCO_3$ for dissolved inorganic carbon (DIC) analysis (Chen et al., 2011). Parameters such as the water temperature (T), pH, EC were measured in situ with an in situ multi-parameter instrument (Multi 350i/SET, Munich, Germany). Major chemistry and isotopes (^{2}H, ^{18}O, ^{3}H and ^{14}C) of the sampled water were analyzed at the Laboratory of Groundwater Sciences and Engineering in the Institute of Hydrogeology and Environmental Geology, Chinese Academy of Geological Sciences (Shijiazhuang, Hebei Province, China). Major cations (K^+, Na^+, Ca^{2+}, Mg^{2+}) were measured by inductively coupled plasma-mass spectrometry (Agilent 7500ce ICP-MS, Tokyo, Japan). Total dissolved solids (TDS) and HCO_3^- were determined by gravimetric analysis and acid-base titration, respectively. Cl^-, SO_4^{2-} and NO_3^- were analyzed using spectrophotometry (PerkinElmer Lambda 35, Waltham, MA, USA). The ionic charge balance of all samples were within 5% difference. $\delta^{18}O$ and $\delta^{2}H$ were measured by isotope ratio mass spectrometry using a Finnigan MAT 253 and reported relative to the Vienna Standard Mean Ocean Water (VSMOW) standard. The analytical errors are ±0.2‰ for $\delta^{18}O$ and ±1.0‰ for $\delta^{2}H$. The tritium content was determined using electrolytic enrichment and liquid scintillation technique (Chen et al., 2011) with the precision of ±0.3 TU. The activity of ^{14}C was analyzed by accelerator mass spectrometry, and expressed as a percentage of modern carbon (pMC). The standard deviation of analytical results ranges between 0.7 pMC and 1.0 pMC.

3.2 Two-dimensional groundwater flow numerical simulation

It is assumed that the variation of density and viscosity of waters could be neglected in most of the flow system (Zone 1~4). For simplicity, groundwater in the terminal lake zone (Zone 5) is also regarded as being mainly driven by gravity. Thus the equation governing variably saturated groundwater flow is as the following (Richards, 1931):

$$\frac{\partial}{\partial t}\emptyset S = \mathrm{div}[K\nabla h]$$

Where ϕ is the porosity, S is the liquid saturation, K is the hydraulic conductivity (m/d), h is the hydraulic head (m). The TOUGH2 code (Transport Of Unsaturated Groundwater and Heat), which has quite robust simulation capabilities, is used to numerically solve this equation (Pruess et al., 1999).

© Author(s) 2017. CC BY 4.0 License.

The cross section parallel to the main direction of groundwater flow in GRW (Fig.1 & 8) was selected for the 2-D flow simulation. This section starts at the mountain pass and ends at the Terminal Lake Dabusun, with an approximate length of 100 km. Boundaries were specified according to the hydrogeology condition. The southern lateral boundary and top boundary in the alluvial fan are defined as given flux boundaries, and the bottom boundary of the section is regard as a zero flux boundary. The springs and evaporation are set as mixed boundaries. The lake boundary in the basin center is specified as a given head boundary.

An irregular discretization was conducted vertically to capture the variation of water table near the ground surface and also implement an efficient simulation. Cells are presented with the minimum thickness of 0.1 m near the ground surface and gradual increasing thickness downward, with a maximum thickness of about 80 m. Equal discretization was applied in the horizontal direction with a horizontal size of 1000 m for one cell. The initial permeability of various lithology are specified based on the borehole drilling records and pumping test results, with the K_h (horizontal hydraulic conductivity) in the range of $10^2 \sim 10^{-3}$ m/d and anisotropy ratio K_h/K_v=5~10 (K_v is vertical hydraulic conductivity). In this study, the model is used to present the flow pattern under equilibrium conditions, thus the recharge rates and hydraulic heads are given according to the annual average values. Evaporation was modeled using a newly developed method described by Hao et al. (2016), and the initial potential evaporation specified is 2600 mm per year. Springs are simulated using the DELV module in TOUGH2, and the productivity index (PI) specified in DELV module is calculated using the following equation (Pruess et al., 1999):

$$\mathrm{PI} = \frac{2\pi(k\Delta z)}{\ln\left(\sqrt{A/\pi}/r\right) + s - 1/2}$$

Where Δz is the layer thickness (m), A is the grid block area (m^2), r is the spring radius (m), s is the skin factor. Annual average observed hydraulic heads are used as natural constraints for the model calibration.

4 Results

4.1 Hydrochemistry and isotopic results for surface and groundwaters

The chemical analysis results of surface water and groundwater samples are presented in Table1. River waters from the mountain pass (Zone 2) to the low-lying depression (Zone 5) are slightly alkaline with a range in pH values from 7.94 to 9.45. Lake water L1, which was sampled from the fresh lake recharged directly by river water in the low-lying depression

© Author(s) 2017. CC BY 4.0 License.

(Zone 5), is also slightly alkaline with a pH value of 8.98. Samples from the salt lakes such as Lake Qarhan, Lake Dabusun are slightly acidic with values range from 6.03 to 6.28. Groundwater in the study area is neutral to slightly alkaline. The shallow phreatic groundwater (SGW) shows an evolving trend from slightly alkaline to slightly acidic along the flow path with the pH varying from 9.34 to 6.03. However, deep confined groundwater (DGW) samples are all slightly alkaline with pH values ranging between 7.83 and 8.69.

Surface water and groundwater present distinct major solute chemistry across the study area. As shown in Table 1, the concentration of ions in river waters demonstrates an increase along the length of the river, with the TDS values varying from 393 mg/L to 2,319 mg/L. This increase has been attributed to increasing evaporation (Wang et al., 2013). Lake waters, except L1 (TDS= 10,937 mg/L), have extremely high TDS values with a mean value of 401,428 mg/L, implying intensive evaporation and potentially a complex hydrogeochemical history, as well as possible multi-water sources outside of Golmud River water (Lowenstein and Risacher, 2009). The surface water types evolve from a HCO_3·Cl-Ca·Mg·Na water type in the alluvial fan area (Zone 2) to Cl-Na, Cl-K-Na and Cl-Mg type in the low-lying central depression (Zone 5) (Fig.2a). Groundwater shows a similar hydrochemical evolution along the flow path. SGW evolves from HCO_3·Cl-Ca·Mg·Na type water with a mean TDS value of 618 mg/L in the alluvial fan (Zone 2) to Cl-Na type with a mean TDS value of 32,029 mg/L in the middle-lower stream area (Zone 4), and eventually to Cl-Mg type with an average TDS value of 348,715 mg/L in the low-lying depression (Zone 5) (Fig.2b). DGW has a similar evolutionary trend as SGW along the groundwater flow path, but it is much fresher when contrasted with the SGW at the same location (Fig.2c), indicating evaporation has had a significant influence on the hydrochemical development of SGW. There is virtually no difference in TDS and composition between SGW and DGW from the central depression (Zone 5), implying extremely long residence times in aquifers and complete reaction with aquifer mediums.

The statistical summary of isotope results for precipitation, river water, lake water and groundwater can be found on Fig.3 and Table 2. The representative snowmelt water in the Kunlun Mountainous area (Zone 1) has a δD value of -77.0 ‰ and $\delta^{18}O$ value of -11.9 ‰. The δD and $\delta^{18}O$ values of precipitation in the mountainous area (Zone 1) are in the range of -85.3 to -71.6 ‰ and -10.9 ‰ to -9.3 ‰, with an average value of -75.2 ‰ and -10.0 ‰, respectively. The δD values of precipitation in the alluvial fan (Zone 2) range from -68.1 ‰ to -66.2 ‰ with the average value of -67.2 ‰ and $\delta^{18}O$ values ranging from -10.1 ‰ to -9.7 ‰ with an average value of -9.9 ‰. The enrichment of stable hydrogen and oxygen isotopes in precipitation from the mountainous area to the basin reflects secondary evaporation effect of precipitation in arid inland areas (Clark and Fritz, 1997). The δD and $\delta^{18}O$ values of river water vary from -75.7 ‰ to -46.7 ‰ and between -11.1 ‰ and -4.8 ‰, respectively, showing a gradual enrichment trend along the river flow path. Fresh and salt lake waters are all significantly enriched in heavy isotopes with values ranging from -27.0 ‰ to -4.0 ‰ for δD and from 0.4 ‰ to 4.5 ‰ for $\delta^{18}O$. As shown on Figure 3 a and b, the SGW from the alluvial fan (Zone 2) to the middle-lower stream area (Zone 4) show an overall gradual enrichment trend along the flow path. In contrast, the DGW shows a significant depletion trend from the south to the north. Groundwater at different depths in the low-lying depression (Zone 5) are all brines with δD values ranging from -66.0 ‰

© Author(s) 2017. CC BY 4.0 License.

to -2.0 ‰ and the $\delta^{18}O$ values ranging between -10.8 ‰ and -0.6 ‰, demonstrating relative enriched characteristics in contrast with the fresher groundwater in the upstream areas.

The ^{3}H values range from 56.3 TU to 12.1 TU in the SGW and from 25.7 TU to <1 TU in the DGW along the groundwater flow path (Fig.3d). The ^{14}C activities in SGW vary from 57.9 pMC to 11.9 pMC, and in DGW range from 49.15 pMC to 0.7 pMC along the flow path (Fig. 3c). The spatial distributions of ^{3}H and ^{14}C results indicate increasing residence times for groundwaters in the aquifers from the south to north. While one shallow phreatic groundwater sample (G215) in the low-lying depression (Zone 5) was observed with relative high ^{3}H content (18.9 TU), this may be caused by the rapid infiltration of surface water in flood period.

4.2 2D groundwater flow modelling

The groundwater flow model was calibrated using annual average hydraulic heads from 63 different shallow wells measured in 2015 along the cross section (not shown on Figure). The calibration shows a good match between simulated and observed hydraulic heads as demonstrated in Fig. 4. The comparison results show that the fit to observed hydraulic heads is better in the loess plain (including Zone 3, 4, 5) with the maximum deviation less than 0.8 m, while relative poor in the alluvial fan (Zone 2) with the maximum deviation less than 5 m. The deviation in the loess plain is mainly caused by the heterogeneity and anisotropy in lithology (Gu et al., 2017). The relative large deviation in results within the alluvial fan is most likely attributed to the steep hydraulic gradient (Islam et al., 2017) and larger seasonal fluctuation of hydraulic heads. Over the whole study area, the RMSE (Root Mean Squared Error) is only 1.57 m, therefore, the calibrated model can be used to reveal the groundwater flow pattern.

The estimated hydraulic parameters are shown in Table 3. The estimated values of K_h are 56.3 m/d for gravel sand, 13.7 m/d for sand, 0.62 m/d for sandy silt, 0.13 m/d for silt and 0.001 m/d for clay. The anisotropy ratio of K_h/K_v was estimated as 10 for gravel sand and sand, and 5 for sandy silt, silt and clay. These parameters are effective values under the assumption of homogeneity in each layer. The water budget analysis indicates a dynamic equilibrium state with the equilibrium difference of 0.62%. Springs are the dominant discharge form, followed by evaporation and lake discharge, accounting for 76.81%, 22.44% and 1.37%, respectively.

5 Discussion

5.1 Water provenance and recharge characteristics

The δD and $\delta^{18}O$ isotope analysis results for different water types are shown on Fig.5a in relation to the Global Meteoric Water Line (GMWL: $\delta D = 8 \times \delta^{18}O + 10$) (Craig, 1961). The Golmud Watershed Local Meteoric Water Line (LMWL: $\delta D = 6.98 \times \delta^{18}O + 9.6$) (Wang, 2014) and Golmud Watershed Local Evaporation Line (LEL) ($\delta D = 4.09 \times \delta^{18}O + 28.1$, R^2=0.94), which is the linear regression line of river and lake water in the study area, are also shown on Fig.5a.

© Author(s) 2017. CC BY 4.0 License.

The slope and intercept of the LMWL (6.98 and 9.6) are lower than those of the GMWL (8 and 10) as a result of secondary evaporation which occurred during precipitation, reflecting the arid climatic characteristics of the study area (Dogramaci et al., 2012; Wang et al., 2017).

As shown in Fig.5a, most of the surface water and groundwaters in the study area are situated close to the GMWL and LMWL, indicating a meteoric origin. However, the spatial distribution of precipitation is extremely uneven. Most of precipitation occurred in the Kunlun mountainous area to the south. Precipitation in the basin is very limited (annual rainfall less than 50 mm) and in this area there is little effective recharge to the aquifers (Xiao et al., 2017). Thus, surface water and groundwater in the study area mainly originates from meteoric water (including precipitation and snowmelt) in the mountainous areas. River water (δD: -75.4~-64.8 ‰, $\delta^{18}O$: -11.1~-9.3 ‰) and groundwater (δD: -65.0 ‰, $\delta^{18}O$: -9.7 ‰) in the mountainous area (Zone 1) have nearly similar stable water isotopic signatures with precipitation (δD: -85.3~-71.6 ‰, $\delta^{18}O$: -10.9~-9.3 ‰) and snowmelt water (δD: -77.0 ‰, $\delta^{18}O$: -11.9 ‰) values from the Kunlun mountainous area (Zone 1), indicating their direct recharge relationship (Fig.5a). River waters flow towards the northern low-lying depression of the central basin, and show a gradual enrichment trend due to intensive evaporation. Lake waters sampled from the low-lying depression (Zone 5) have the most enriched stable water isotope values, and lie at the end of LEL defined by progressive evaporative enrichment of river water samples (Fig.5b).

The δD and $\delta^{18}O$ values of the SGW and DGW demonstrate different varying trends along the groundwater flow path. The SGW shows a gradual positive enrichment trend in heavy isotopes along the LEL (Fig.5c), implying the influence of evaporation. For the alluvial fan (Zone 2), the δD and $\delta^{18}O$ values of groundwater are very similar to that of river water in the alluvial fan (Zone 2) and groundwater in the mountainous area (Zone 1) (Table 2), indicating groundwater in the alluvial fan (Zone 2) is recharged directly by the seepage of river water and lateral inflow from the mountainous area. This is confirmed by similarities in major chemical composition (Fig.2). The similar stable isotopic values also signify groundwater in the alluvial fan (Zone 2) has a short residence time, which is corroborated by elevated ^{3}H (20.0~56.3 TU, mean value of 35.5 TU) indicating the residence time is less than 60 years based on ^{3}H data (Xiao et al., 2017). SGW in the overflow zone (Zone 3) and the middle-lower stream area (Zone 4) also have similar δD and $\delta^{18}O$ values as the river waters in the same area (Table 2), implying SGW has a very close hydraulic relationship with the rivers. The ^{3}H values of the SGW in Zone 3 and Zone 4, range from 12.1 TU to 25.7 TU and from 14.4 TU to 17.5 TU, respectively, with the mean value of 21.1 TU and 16.0 TU, suggest that SGW in these two zones contain a large component of modern water or mixtures of old and modern water.

DGW in the overflow zone (Zone 3) and the middle-lower stream area (Zone4) are observed to have a completely opposite evolution trend in that the δD and $\delta^{18}O$ values become more depleted along the groundwater flow path (Fig.5d). The depleted nature of the δD and $\delta^{18}O$ values may have two interpretations: (1) these aquifers have another recharge region where rainfall with low δD and $\delta^{18}O$ values occurs; or (2) the groundwater is ancient water recharged under colder climatic conditions (Chen et al., 2012; Awaleh et al., 2017). If (1) is the reason that groundwater would be more depleted in δD and $\delta^{18}O$ along the groundwater flow paths, it is difficult to construct a mixing model that would supply more depleted waters along the

© Author(s) 2017. CC BY 4.0 License.

deep flow path. According to the groundwater age estimated using ^{14}C (calculated by Tamers model (Tamers, 1975; Chen et al., 2003) and a statistical correction model (Verhagen et al., 1974; Geyh et al., 2000)), the DGW in Zone 3 and Zone 4 was recharged from 2,030 years B.P. to more than 20,090 years B.P. (Holocene to late Pleistocene), which was a period when the climate changed from cold and wet condition (30,000 years B.P. to 17,000 years B.P.) to warm and dry condition (14,000 years B.P. to present) (Zhang et al., 2011). Consequently, it is believed that the depleted δD and $\delta^{18}O$ waters in the DGW were recharged by paleo water under a colder climate relative to present. Similar findings were reported in the adjoining Nomhon watershed of Qaidam Basin (Xiao et al., 2017). Additionally, this is consistent with the paleo-climate findings recorded using groundwater data from other basins of NW China (He et al., 2015; Huang et al., 2017).

Groundwater in the low-lying depression area (Zone 5), regardless of depth, are all brines with TDS values greater than 100,000 mg/L. Given the tectonic activity and depocenter migration within the Qaidam Basin over geological history (Chen and Bowler, 1986), groundwater in the low-lying depression area (Zone 5) has a large component of paleo-brines migrated from western Qaidam Basin due to the uplift in the past. According to the ^{14}C age of DGW in Zone 4, the deduced age of DGW in the low-lying depression (Zone 5) is more than 20,000 years. SGW was observed with high ^{3}H content (18.9 TU) adjacent to the Terminal lake (G217) (Fig.1 and Table 2), indicating mixing with leakage of modern surface water. As shown in Fig.5a, most groundwaters in the basin center show a considerable deuterium excess, indicating that the original precipitation waters experienced considerable evaporation and vapor re-equilibration during recharge.

5.2 Mechanisms controlling hydrochemistry

Generally, the composition of natural groundwater is primarily controlled by the chemical composition of recharge waters, water-aquifer matrix interaction, and groundwater residence time (Redwan and Moneim, 2015; Verma et al., 2016). As exhibited in the diagrams between TDS vs. $Na^+/(Na^+ + Ca^{2+})$ and $Cl^-/(Cl^- + HCO_3^-)$ (Fig.6), the major mechanisms controlling groundwater chemistry are water-rock interaction and evaporation-mineral precipitation processes (Gibbs, 1970). Water-rock interaction processes dominant the controls on groundwater chemistry at all depths in Zone 2 due to the great depth and the negligible impact of evaporation. For the overflow zone (Zone 3) and the middle-lower stream area (Zone 4), the governing mechanisms for SGW change from water-rock interaction to evaporation-mineral precipitation due to the gradual decrease of groundwater depth and recharge inputs from waters having undergone the influence of intensive evaporation in that part of the basin. Nearly all DGW in this part of the flow system are controlled by water-rock interaction. Two DGW samples are observed to plot in the evaporation-crystallization domain (Fig.6). This is due to a high TDS and over-saturation of evaporative minerals in the groundwater resulting in mineral precipitation (crystallization). For the low-lying depression (Zone 5), evaporation has a significant influence on the chemistry of SGW, and crystallization (precipitation) of many mineral phases is the primary geochemical process controlling both the SGW and DGW chemistry.

In order to further constrain the sources of solute in groundwater, the relationships between various ions are compared (Fig.7). The relation of Na^+ vs. Cl^- shows both SGW and DGW from the piedmont to the middle-lower stream area (Zone 2, 3, 4) are plotted along the 1:1 line (Fig.7a), suggesting that halite dissolution is potentially a primary process/source of Na^+

© Author(s) 2017. CC BY 4.0 License.

and Cl^- mineralization in groundwater. The calculated results of halite saturation index (SI_{halite}<0) (Table 4) confirm that halite minerals of the aquifer matrix could be readily available to enter the water. In addition, core drilling demonstrated that evaporate salts such as halite, calcium sulfate and sodium sulfate are widespread in the aquifer materials, and can provide the solute source. Some of SGW in Zone 4 are observed with the Na^+ excess relative to Cl^-, while groundwater, regardless of the depth, shows deficiency of Na^+ with respect of Cl^-, implying the existence of some other processes contributing Na^+ not Cl^- to groundwater and changing the ratio of Na^+/Cl^-.

One explanation for the excess of Na^+ would be that the abundant Ca^{2+} and Mg^{2+} in fresh groundwater exchanges with the Na^+ on the surface of clay minerals, which results in an increase of Na^+ concentration and a decrease of Ca^{2+} and Mg^{2+} concentration in groundwater (Awaleh et al., 2017). The relationship of [(Ca^{2+}+Mg^{2+})-(HCO_3^-+SO_4^{2-})] vs. [(Na^++K^+)-Cl^-] (Fig.7f) shows a regression line of $y = 1.0016x + 4.9078, R^2 = 0.9966$ and corroborates the contribution of cation exchange ($Ca^{2+}\ or\ Mg^{2+} + 2NaX\ (solid) \rightarrow 2Na^+ + CaX_2\ or\ MgX_2\ (solid)$) (Verma et al., 2016). In addition, silicate weathering (e.g. $2NaAlSi_3O_8\ (Albite) + 2CO_2 + 11H_2O \rightarrow 2Na^+ + Al_2Si_2O_5(OH)_5\ (Kaolinite) + 3H_4SiO_4 + 2HCO_3^-$) in the aquifers could also contribute Na^+ not Cl^- to groundwater (Guo et al., 2015). The ratio of $Na^+/(Cl^-+SO_4^{2-})$ is around 1 (Fig.7b), demonstrating mirabilite ($Na_2SO_4{\cdot}10H_2O$) dissolution ($Na_2SO_4 \cdot 10H_2O \rightarrow 2Na^+ + SO_4^{2-}$) is an additional strong possible process that could also be responsible for the excess of Na^+ compared to Cl^- in groundwater (Jia et al., 2017). Groundwater in the basin with extremely high TDS concentration (more than 1000,000 mg/L) has very low ratios of Na^+/Cl^- as the result of reverse cation exchange ($Na^+ + CaX_2$ (solid) or MgX_2 (solid) $\rightarrow 2Na^+ + CaX_2$ or MgX_2 (solid)) (Fig.7f).

The relationship between (Ca^{2+}+Mg^{2+}) and (HCO_3^-+SO_4^{2-}) shows that almost all groundwater from the piedmont to the middle-lower stream area (Zone 2, 3, 4) are plotted along the 1:1 line (Fig.7c), implying the dissolution of gypsum, anhydrite, aragonite, calcite and dolomite is the potential ions sources of groundwater in the mineralization process (Dogramaci et al., 2012). As shown in Fig.7d, nearly all groundwater data plot away from the equiline of (Ca^{2+}+Mg^{2+}) vs. HCO_3^-, indicating that the Ca^{2+}, Mg^{2+} and HCO_3^- are not primarily derived from the dissolution of aragonite, calcite and dolomite. The saturation index values of aragonite, calcite and dolomite are almost greater than 0 in all samples (Table 4), suggesting the dissolution of these three minerals must be minimal. While the saturation index values of gypsum and anhydrite for groundwater in these areas are all below zero (Table 4), corroborating the contribution of gypsum and anhydrite dissolution for groundwater mineralization. The deficiency of Ca^{2+} compared to SO_4^{2-} of groundwater presented in Fig.7e is most likely as a result of the aforementioned mirabilite ($Na_2SO_4{\cdot}10H_2O$) dissolution and cation exchange.

Groundwater in the low-lying depression (Zone 5) has extremely high TDS values (Table 1) and almost all minerals are over-saturation (Table 4), therefore, precipitation (crystallization) of minerals is the primary geochemical process in this part of the aquifers (Li et al., 2010). In addition, reverse cation exchange interaction and evaporation, which can be confirmed by the relationship of [(Ca^{2+}+Mg^{2+})-(HCO_3^-+SO_4^{2-})] vs. [(Na^++K^+)-Cl^-] (Fig.7f) and the relation of stable water isotopes (Fig. 4), respectively, are also important mechanisms governing groundwater chemistry. Surface water has significant influence on the geochemical processes that occurred in the shallow aquifers. In the wet season, a large amount of relative fresh water can

© Author(s) 2017. CC BY 4.0 License.

reach the low-lying depression area (Zone 5) and infiltrate to the shallow aquifers. This would dilute the groundwater and dissolve the evaporate salts in the aquifers.

5.3 Groundwater flow and hydrogeochemiscal evolution

Theoretically, three types of groundwater flow systems, namely local, intermediate and regional, may occur in a large basin, and each flow system has its own characteristics based on aspects of flow path, recharge origin, cycle depth, cycle amount, residence time, discharge position, hydrochemistry and controlling mechanisms (Toth, 1963). The cross-sectional groundwater flow modelling results demonstrated the groundwater flow paths in the study area are strictly controlled by distribution of the lithology (Fig.8). Groundwater flow lines are shown to be upward convex in shape at the front of the alluvial fan and the middle-stream area due to an increase in relatively poor permeability due to the addition of finer permeable stratigraphic material. Based on the distribution of flow lines, three groundwater flow systems including local, intermediate and regional system were identified in the study area (Fig.8).

The local groundwater flow system occurs in the shallow part of the alluvial fan (Zone 2) and overflow zone (Zone 3) with the deepest cycle depth within 250 m of surface. This flow system obtains recharge water along the Golmud River flow path and discharges at the overflow zone. The water cycle quantity of the local system estimated by modeling accounts for 82.69% of the total quantity of groundwater in the watershed. Groundwater chemistry is mainly controlled by water-rock interaction and there appears to be very little evaporation. Groundwater has a rapid velocity in this part of the system with the residence time less than 60 a. As a result, groundwater here is fresh with the TDS less than 1000 mg/L and water type mainly HCO_3·Cl-Ca·Mg·Na. This system is the main source of water supply for Golmud city.

The intermediate flow system occurs below the local system and is recharged by river water seepage near the upper part of the alluvial fan. Groundwater flows to lower elevations towards the north and reaches its deepest cycle depth near 600 m at the middle part of the alluvial fan (Zone 2). Due to the increase of aquitards, water flow lines are presented as upward convex shapes at the middle-lower part of alluvial fan (Zone 2). Groundwater flow is constrained by two continuous aquitards (clay layers) at depths of 60 m and 290 m (Fig.8), respectively, at the front of the alluvial fan and overflow zone. The intermediate flow system discharges between the lower overflow zone (Zone 3) and the middle-lower stream area (Zone 4) as evidenced by springs and surface evaporation. The total cycle water quantity of the intermediate system accounts for 14.26% of the total cycle groundwater amount in the watershed. Aquifers of this system in the alluvial fan have higher renewal rates due to their increased permeability, compared to those in the lower overflow zone (Zone 3) and the middle-lower stream area (Zone 4) that have relative low renewal rates as the result of fine lithology with groundwater residence times of about 4,000 years. Hydrochemistry is dominantly controlled by water-rock interaction, and also strongly influenced by evaporation within the discharge area. Because of the short residence time and a shortage of chemical solutes in the aquifers medium, groundwater in the alluvial fan (Zone 2) generally maintains the recharge water chemical characteristics which are fresh and HCO_3·Cl-Ca·Mg·Na type. Sufficient solutes in the aquifer medium and intensive evaporation in the fine soil plain results in groundwater gradually evolving to be brackish water and even some saline waters.

© Author(s) 2017. CC BY 4.0 License.

The regional groundwater flow system occurs under the intermediate system and is recharged at the upper part of the alluvial fan by river water seepage and lateral flow within the mountainous area and discharges at the basin center into terminal lakes resulting in evaporation. Groundwater flow paths are significantly controlled by the lithology (Fig.8), and divided from the intermediate system by the continuous aquitard at a depth of 290 m. Aquifers of this system have very low renewal rates with residence times up to and greater than 20,000 years. The modelled cycle water quantity of the regional system is only 3.05%. Groundwater chemistry is mainly influenced by water-rock interaction in this system, except for that of shallow aquifers in discharge area (Zone 5) which are strongly influenced by evaporation. Due to the substantial difference of residence time, water-rock interaction results in different hydrochemical characteristics from the other aquifer system. Groundwater that was presented as fresh water with a dominant water type of HCO_3·Cl-Ca·Mg·Na in the alluvial fan (Zone 2) and overflow zone (Zone 3), become a brackish water type (HCO_3·Cl- Na) and a saline water type (Cl-Na) in the middle-lower stream area (Zone 4), and has evolved to be a brine water type mainly composed of Cl-Mg in the low-lying discharge area (Zone 5).

6 Conclusions

Hydrochemistry, isotopes and 2-dimentional groundwater flow modelling were used to obtain insight into the origin, flow regime and hydrogeochemical evolution of groundwater in a typical arid endorheic watershed in Qaidam Basin, Tibetan plateau. A number of key findings have come out of this study.

The groundwater in the basin originates from precipitation and melt water in the mountainous areas to the south. Groundwater in the alluvial fan is recharged directly by modern river water seepage and mountainous lateral inflow, and has a rapid flow rate. Shallow phreatic waters in the overflow zone and the middle-lower stream area are supported by local and intermediate groundwater flow systems, and have a close chemical and isotopic relationship with surface water. Deep confined groundwater in the overflow zone and the middle-lower stream area are recharged from paleo meteoric water during the late Pleistocene and Holocene under a cold climate based on stable water isotopic data results. Groundwater in the low-lying depression (basin center) is ancient brines possibly migrated from the western Qaidam Basin due to the uplift of the western basin in the geological past. Shallow phreatic aquifers in the low-lying depression (basin center) are also seasonally recharged by modern surface water during flooding periods.

Groundwater in the study area evolves from fresh water to brine water along the flow path. The hydrochemistry of groundwater in the alluvial fan is dominantly controlled by mineral dissolution and cation exchange, and occurs as slightly alkaline water with the TDS values less than 1000 mg/L and a water type with a composition of HCO_3·Cl-Ca·Mg·Na. Deep confined groundwater chemistry in the overflow zone and middle-lower stream area is also controlled by mineral dissolution and cation exchange, as a result of longer residence times in the aquifers, and shows a trend evolving from fresh water to brackish water and finally saline water with increasing solute inputs along the flow paths. As well as water-rock interaction, shallow phreatic water is also affected by intensive evaporation, and therefore, these waters can be much saltier than deep

© Author(s) 2017. CC BY 4.0 License.

confined water. Groundwater in the low-lying depression (basin center) is brine water and the mineral precipitation coupled with reverse cation exchange are the dominant geochemical processes controlling water chemistry. Evaporation is also one of the important geochemical processes in the shallow phreatic aquifers, which can accelerate evaporate mineral precipitation. Salt dissolution occasionally occurred in the low-lying depression (basin center) during flood periods due to the infiltration of large amounts of fresh surface water.

Three different hierarchical groundwater flow systems were identified using the cross-sectional model. The continuous aquitards at depths of 60 m, 290 m and 450 m have significant constraints on groundwater flow. The local flow system occurs in the shallow part of the alluvial fan and overflow zone and discharges in the overflow zone with the deepest cycle depth within 250 m of surface. The intermediate system occurs below the local system and discharges in the lower overflow zone and middle-lower stream area with the deepest cycle depth reaching 600 m below surface. The regional system was divided from the intermediate system by the continuous aquitard at a depth of 290 m and discharge in the low-lying depression (basin center). The discharge water quantity of these three systems accounts for 82.69%, 14.26% and 3.05%, respectively.

This study enhanced the understanding of the origin, flow regime and hydrochemical evolution and controlling mechanisms of the regional groundwater in the Qaidam Basin. These results can provide fundamental information for coping with the future issues such as water conflicts, salt lake exploitation and climate warming in the basin, and also provide references for understanding the hydrogeological processes in other similar endorheic watersheds of northwest China and elsewhere in the world.

Acknowledgements. This work was supported by the National Key R&D Program of China [2017YFC0406106] and the China Geological Survey [DD20160291]. We appreciate the help of Xiangzhi You at Xi'an Center of Geological Survey, China Geological Survey, Qichen Hao at the Institute of Hydrogeology and Environmental Geology, Chinese Academy of Geological Sciences, and Xiaomin Gu, Jingxing Liu and Dong Wang at China University of Geosciences (Beijing).

References

Anderson, M.P., Woessner, W.W., Hunt, R.J., 2015. Applied groundwater modeling : simulation of flow and advective transport. Academic Press.

Awaleh, M.O. et al., 2017. Recharge, groundwater flow pattern and contamination processes in an arid volcanic area: Insights from isotopic and geochemical tracers (Bara aquifer system, Republic of Djibouti). Journal of Geochemical Exploration, 175: 82-98. DOI:https://doi.org/10.1016/j.gexplo.2017.01.005

Bredehoeft, J.D., Konikow, L.F., 2012. Ground-water models: validate or invalidate. Groundwater, 50(4): 493.

© Author(s) 2017. CC BY 4.0 License.

Chen, A., Zheng, M., Shi, L., Wang, H., Xu, J., 2017. Magnetostratigraphy of deep drilling core 15YZK01 in the northwestern Qaidam Basin (NE Tibetan Plateau): Tectonic movement, salt deposits and their link to Quaternary glaciation. Quaternary International, 436: 201-211. DOI:http://dx.doi.org/10.1016/j.quaint.2017.01.026

Chen, J. et al., 2012. Isotopic constraints on the origin of groundwater in the Ordos Basin of northern China. Environmental Earth Sciences, 66(2): 505-517. DOI:10.1007/s12665-011-1259-6

Chen, K., Bowler, J.M., 1986. Late pleistocene evolution of salt lakes in the Qaidam basin, Qinghai province, China. Palaeogeography Palaeoclimatology Palaeoecology, 54(1-4): 87-104.

Chen, L., Ma, T., Ma, J., Du, Y., Xiao, C., 2015. Identification of material source for the salt lakes in the Qaidam Basin. hydrogeology & Engineering Geology, 42(4): 101-107.

Chen, Z. et al., 2003. Paleoclimatic interpretation of the past 30 ka from isotopic studies of the deep confined aquifer of the North China plain. Applied Geochemistry, 18(7): 997-1009.

Chen, Z., Wei, W., Liu, J., Wang, Y., Chen, J., 2011. Identifying the recharge sources and age of groundwater in the Songnen Plain (Northeast China) using environmental isotopes. Hydrogeology Journal, 19(1): 163-176.

Clark, I.D., Fritz, P., 1997. Environmental Isotopes in Hydrogeology. CRC press, New York.

Craig, H., 1961. Isotopic Variation in Meteoric Waters. 133(3465): 1702-1703.

Dogramaci, S., Skrzypek, G., Dodson, W., Grierson, P.F., 2012. Stable isotope and hydrochemical evolution of groundwater in the semi-arid Hamersley Basin of sub-tropical northwest Australia. Journal of Hydrology, 475(26): 281-293.

Edmunds, W.M., Ma, J., Aeschbach-Hertig, W., Kipfer, R., Darbyshire, D.P.F., 2006. Groundwater recharge history and hydrogeochemical evolution in the Minqin Basin, North West China. Applied Geochemistry, 21(12): 2148-2170. DOI:http://dx.doi.org/10.1016/j.apgeochem.2006.07.016

Geyh, M. et al., 2000. groundwater saturated and unsaturated zone. Environmental isotopes in the hydrological cycle: Principles and Applications, 4. UNESCO & IAEA, Vienna.

Gibbs, R.J., 1970. Mechanisms Controlling World Water Chemistry. Science, 170(3962): 1088.

Gu, X., Shao, J., Cui, Y., Hao, Q., 2017. Calibration of two-dimensional variably saturated numerical model for groundwater flow in arid inland basin, China. Current science, 113(3): 403-412.

Guo, X. et al., 2015. Stable isotopic and geochemical identification of groundwater evolution and recharge sources in the arid Shule River Basin of Northwestern China. Hydrological Processes, 29(22): 4703-4718.

Hao, Q., Shao, J., Cui, Y., Zhang, Q., 2016. Development of a new method for efficiently calculating of evaporation from the phreatic aquifer in variably saturated flow modeling. Journal of Groundwater Science and Engineering, 4(1): 26-34.

He, J., Ma, J., Zhao, W., Sun, S., 2015. Groundwater evolution and recharge determination of the Quaternary aquifer in the Shule River basin, Northwest China. Hydrogeology Journal, 23(8): 1745-1759. DOI:10.1007/s10040-015-1311-9

Herrera, C. et al., 2016. Groundwater flow in a closed basin with a saline shallow lake in a volcanic area: Laguna Tuyajto, northern Chilean Altiplano of the Andes. Science of The Total Environment, 541: 303-318. DOI:http://dx.doi.org/10.1016/j.scitotenv.2015.09.060

© Author(s) 2017. CC BY 4.0 License.

Hou, X., Zhang, J., Liu, J., 2014. Assessment of Groundwater Source of Piedmont Plain Area of China Northwest Arid Region Based On Numerical Modeling. Acta Geologica Sinica, 88(s1): 419–420.

Huang, G., Chen, Z., Sun, J., Wang, J., Hou, Q., 2016. Groundwater quality in aquifers affected by the anthropogenic and natural processes in an urbanized area, south China. Environmental Forensics, 17(1): 107-119.

Huang, T., Pang, Z., Li, J., Xiang, Y., Zhao, Z., 2017. Mapping groundwater renewability using age data in the Baiyang alluvial fan, NW China.

Islam, M.B. et al., 2017. A regional groundwater-flow model for sustainable groundwater-resource management in the south Asian megacity of Dhaka, Bangladesh. Hydrogeology Journal, 25(3): 617-637. DOI:10.1007/s10040-016-1526-4

Jia, Y. et al., 2017. Sources of groundwater salinity and potential impact on arsenic mobility in the western Hetao Basin, Inner Mongolia. Science of the Total Environment, 601-602: 691.

Jiang, X.W. et al., 2014. Field identification of groundwater flow systems and hydraulic traps in drainage basins using a geophysical method. Geophysical Research Letters, 41(8): 2812–2819.

Jiao, J.J., Zhang, X., Yi, L., Kuang, X., 2015. Increased Water Storage in the Qaidam Basin, the North Tibet Plateau from GRACE Gravity Data. Plos One(10). DOI:10.1371/journal.pone.0141442

Li, M. et al., 2010. Evaporite minerals and geochemistry of the upper 400 m sediments in a core from the Western Qaidam Basin, Tibet. Quaternary International, 218(1–2): 176-189.

Lowenstein, T.K., Risacher, F., 2009. Closed Basin Brine Evolution and the Influence of Ca–Cl Inflow Waters: Death Valley and Bristol Dry Lake California, Qaidam Basin, China, and Salar de Atacama, Chile. Aquatic Geochemistry, 15(1): 71-94.

Pruess, K., Oldenburg, C., Moridis, G., 1999. TOUGH2 user's guide version 2. Lawrence Berkeley National Laboratory.

Redwan, M., Moneim, A.A.A., 2015. Factors controlling groundwater hydrogeochemistry in the area west of Tahta, Sohag, Upper Egypt. Journal of African Earth Sciences, 118: 328-338.

Richards, L.A., 1931. Capillary conduction of liquids through porous mediums. Physics, 1(5): 318-333.

Su, X., Xu, W., Yang, F., Zhu, P., 2015. Using new mass balance methods to estimate gross surface water and groundwater exchange with naturally occurring tracer 222Rn in data poor regions: a case study in northwest China. Hydrological processes, 29(6): 979-990.

Tóth, Á. et al., 2016. Groundwater flow pattern and related environmental phenomena in complex geologic setting based on integrated model construction. Journal of Hydrology, 539: 330-344.

Tamers, M.A., 1975. Validity of radiocarbon dates on ground water. Geophysical surveys, 2(2): 217-239. DOI:10.1007/BF01447909

Tan, H. et al., 2009. Chemical and Isotopic Approach to Groundwater Cycle in Western Qaidam Basin,China. Chinese Geographical Science, 19(4): 357-364.

Tan, H., Rao, W., Ma, H., Chen, J., Li, T., 2011. Hydrogen, oxygen, helium and strontium isotopic constraints on the formation of oilfield waters in the western Qaidam Basin, China. Journal of Asian Earth Sciences, 40(2): 651-660.

© Author(s) 2017. CC BY 4.0 License.

Toth, J., 1963. A theoretical analysis of groundwater flow in small drainage basins. Journal of Geophysical Research, 68(16): 4795-&. DOI:10.1029/JZ068i008p02354

Toth, J., 1980. Cross-formational gravity-flow of groundwater: a mechanism of the transport and accumulation of petroleum (the generalized hydraulic theory of petroleum migration).

Vengosh, A. et al., 1995. Chemical and boron isotope compositions of non-marine brines from the Qaidam Basin, Qinghai, China. Chemical Geology, 120(1): 135-154.

Verhagen, B.T., Mazor, E., Sellschop, J.P.F., 1974. Radiocarbon and tritium evidence for direct rain recharge to ground waters in the northern Kalahari. Nature, 249(5458): 643-644.

Verma, S., Mukherjee, A., Mahanta, C., Choudhury, R., Mitra, K., 2016. Influence of geology on groundwater–sediment interactions in arsenic enriched tectono-morphic aquifers of the Himalayan Brahmaputra river basin. Journal of Hydrology, 540: 176-195.

Wang, D., Ren, F., 1996. Abnormal Groundwater Chemistry in Ge'ermu Allubium Aquifer and its Origin. Journal of Changchun University of Earth Sciences, 26(2): 191-195.

Wang, L., Dong, Y., Xu, Z., Qiao, X., 2017. Hydrochemical and isotopic characteristics of groundwater in the northeastern Tennger Desert, northern China. Hydrogeology Journal(1–2).

Wang, P., Yu, J., Zhang, Y., Liu, C., 2013. Groundwater recharge and hydrogeochemical evolution in the Ejina Basin, northwest China. Journal of Hydrology, 476: 72-86. DOI:https://doi.org/10.1016/j.jhydrol.2012.10.049

Wang, Y., 2014. Geochemistry Evolution and Water Cycle Patterns of Groundwater in Golmud River Basin, Chang'an University, Xi'an, China.

Wang, Y. et al., 2010. Use of Rushed Deep Lacustrine Freshwater in the Plain Area of Qaidam Basin. Northwestern Geology, 43(3): 113-119.

Xiao, Y., Shao, J., Cui, Y., Zhang, G., Zhang, Q., 2017. Groundwater circulation and hydrogeochemical evolution in Nomhon of Qaidam Basin, northwest China. Journal of Earth System Science, 126(2): 1-15. DOI:10.1007/s12040-017-0800-8

Xu, W. et al., 2017. Multi-tracer investigation of river and groundwater interactions: a case study in Nalenggele River basin, northwest China.

Ye, C. et al., 2014. Hydrochemistry of the Gasikule Salt Lake,Western Qaidam Basin of China. Acta Geologica Sinica, 88(s1): 170-172.

Zhang, J., 2013. Groundwater resource evoluation of Xiangride-Nuomuhong Piedmont Plain, China University of Geosciences (Beijing), Beijing, China.

Zhang, M. et al., 2011. Sedimental features and paleo-environment reconstruction of the slope deposit at Xiaogangou of the Golmud River. Arid Land Geography, 34(6): 890-903.

Zheng, M., Tang, J., Liu, J., Zhang, F., 1993. Chinese saline lakes. Hydrobiologia, 267(1): 23-36. DOI:10.1007/bf00018789

Hydrol. Earth Syst. Sci. Discuss., https://doi.org/10.5194/hess-2017-647
Manuscript under review for journal Hydrol. Earth Syst. Sci.
Discussion started: 21 November 2017
© Author(s) 2017. CC BY 4.0 License.

Hydrology and Earth System Sciences
Discussions

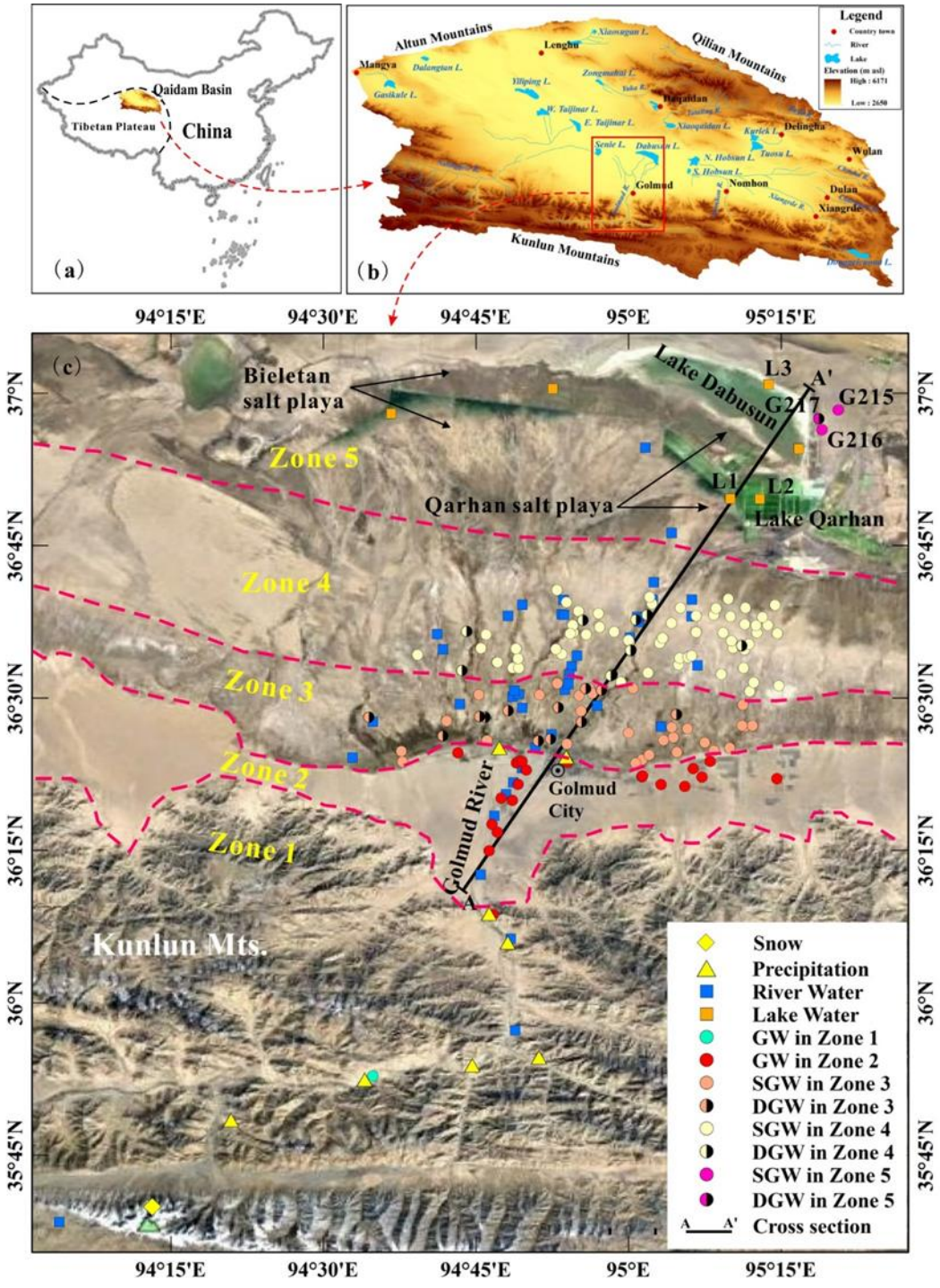

Figure 1: Location of the study area (a) within China, (b) within the Qaidam Basin, (c) details of sampling location and groundwater/physiographic zones within the study area.

Hydrol. Earth Syst. Sci. Discuss., https://doi.org/10.5194/hess-2017-647
Manuscript under review for journal Hydrol. Earth Syst. Sci.
Discussion started: 21 November 2017
© Author(s) 2017. CC BY 4.0 License.

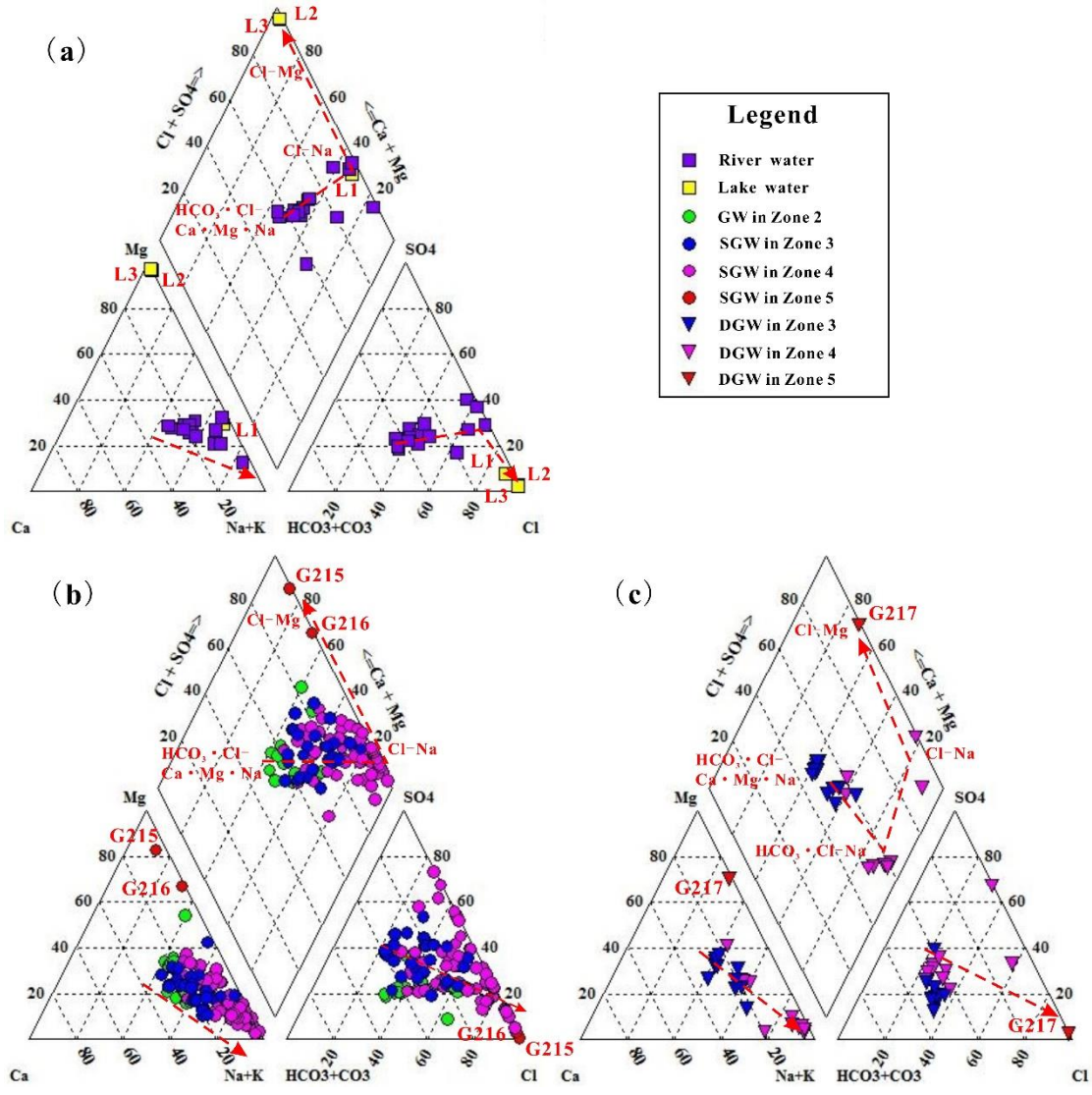

Figure 2: Piper diagrams of sampled surface water and groundwater. (a) surface waters; (b) shallow phreatic groundwaters; (c) deep confined groundwaters from the Qaidam Basin, China. (Red dashed lines and arrows indicate the direction of evolutionary flow systems).

Hydrol. Earth Syst. Sci. Discuss., https://doi.org/10.5194/hess-2017-647
Manuscript under review for journal Hydrol. Earth Syst. Sci.
Discussion started: 21 November 2017
© Author(s) 2017. CC BY 4.0 License.

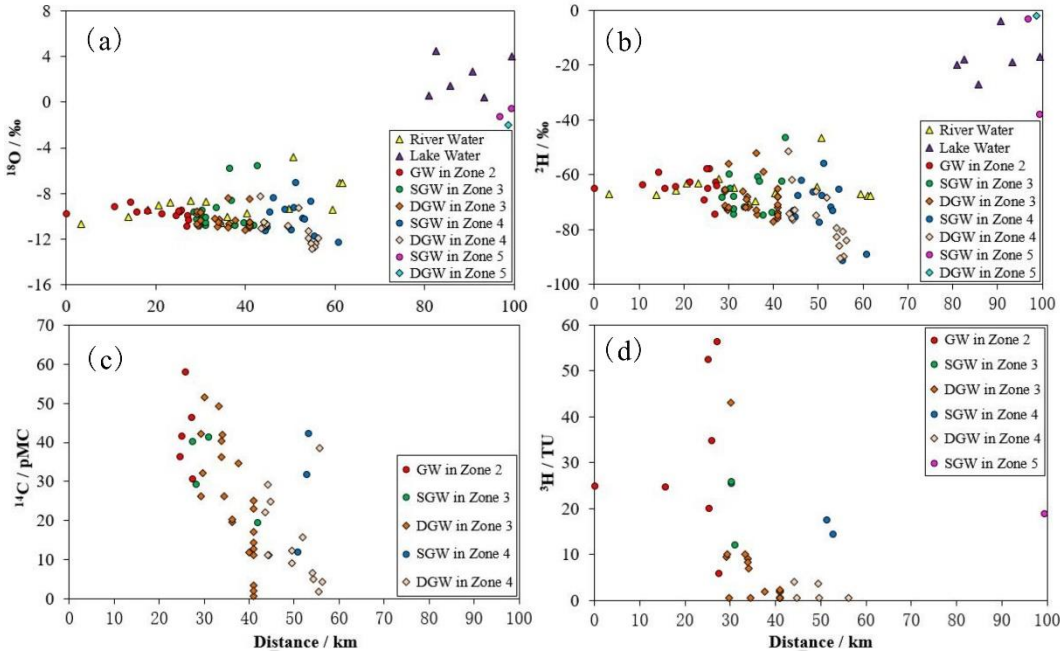

Figure 3: Isotopic data versus distance from the mountain pass along the groundwater flow paths. (a) ^{18}O vs. distance, (b) ^{2}H vs. distance, (c) ^{14}C vs. distance, (d) ^{3}H vs. distance.

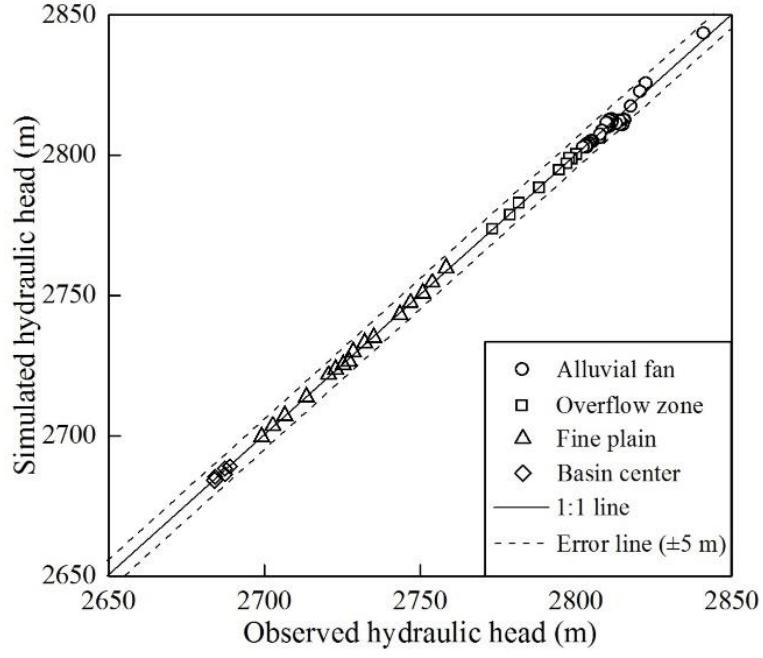

Figure 4: Comparison of observed and simulated hydraulic head values along the groundwater flow system, Golmud Watershed, China.

Hydrol. Earth Syst. Sci. Discuss., https://doi.org/10.5194/hess-2017-647
Manuscript under review for journal Hydrol. Earth Syst. Sci.
Discussion started: 21 November 2017
© Author(s) 2017. CC BY 4.0 License.

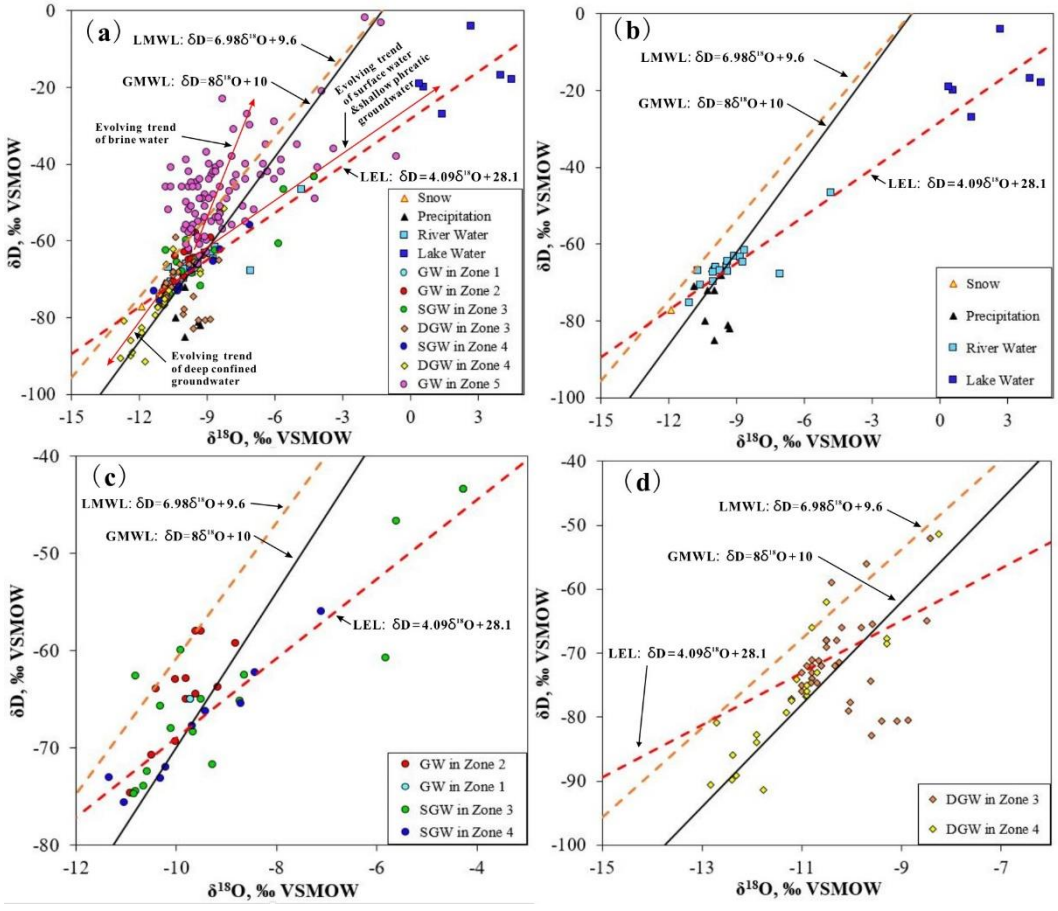

Figure 5: $\delta^{18}O$ vs. δD diagram of precipitation, surface water and groundwater for the Golmud study area of the Qaidam Basin, China. (a) All data, (b) Snow, precipitation and surface waters, (c) Shallow phreatic waters, (d) Deep confined waters.

Hydrol. Earth Syst. Sci. Discuss., https://doi.org/10.5194/hess-2017-647
Manuscript under review for journal Hydrol. Earth Syst. Sci.
Discussion started: 21 November 2017
© Author(s) 2017. CC BY 4.0 License.

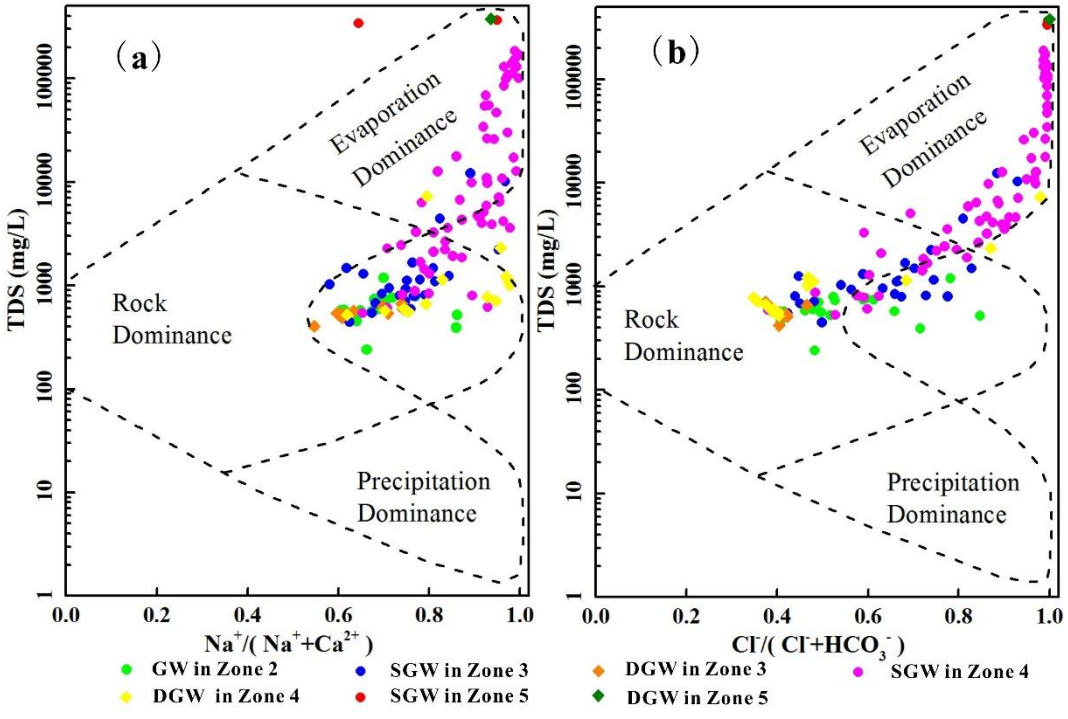

Figure 6: Diagrammatic representation showing the mechanisms controlling groundwater chemistry. (a) TDS vs. $Na^+/(Na^+ + Ca^{2+})$; (b) TDS vs. $Cl^-/(Cl^- + HCO_3^-)$ (after Gibbs, 1970).

Hydrol. Earth Syst. Sci. Discuss., https://doi.org/10.5194/hess-2017-647
Manuscript under review for journal Hydrol. Earth Syst. Sci.
Discussion started: 21 November 2017
© Author(s) 2017. CC BY 4.0 License.

Hydrology and Earth System Sciences
Discussions

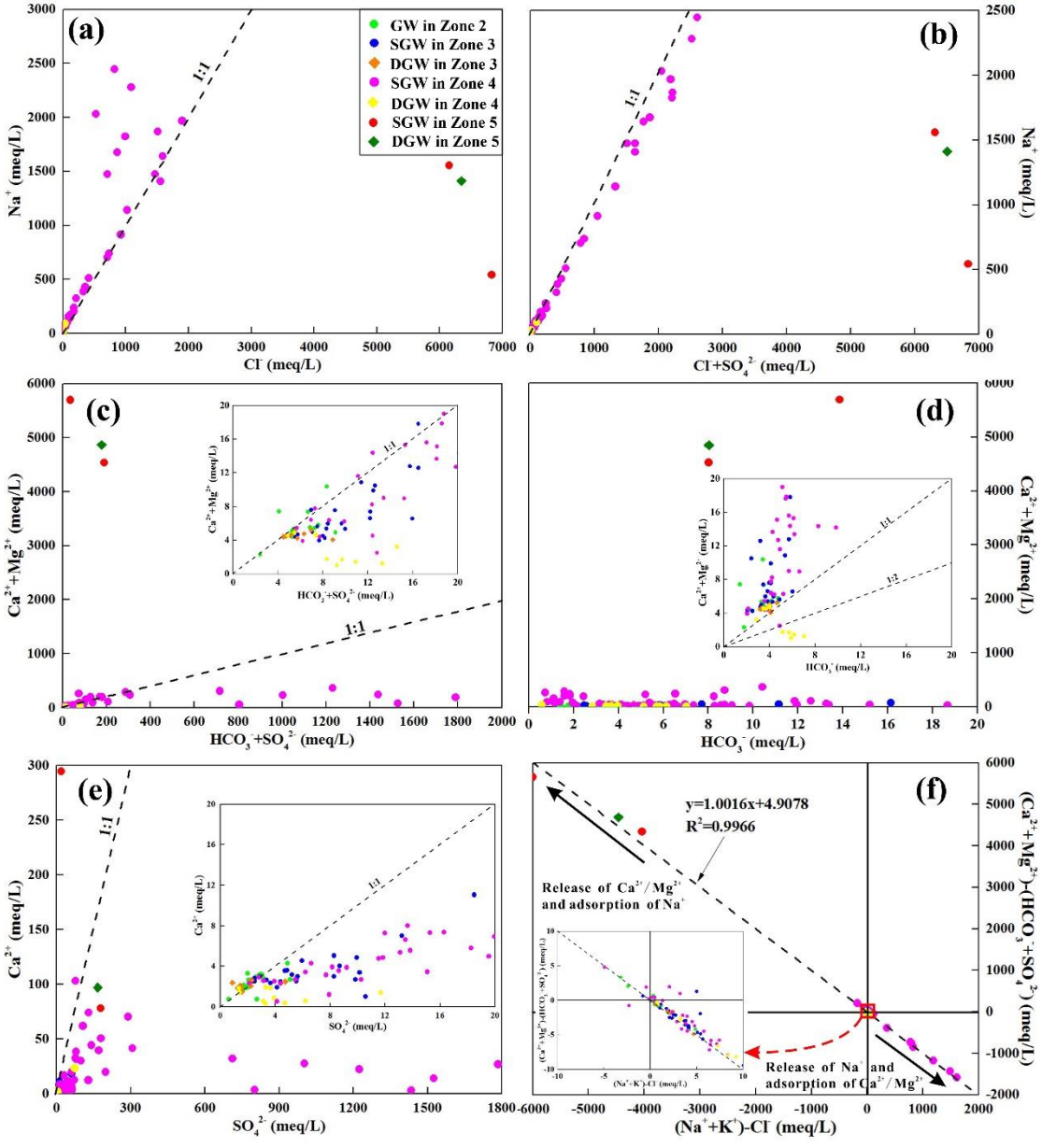

Figure 7: Bivariate plots (meq/L) of various ions in shallow phreatic and deep confined groundwater showed state (a) Na vs. Cl, (b) Na vs. ($Cl+SO_4$), (c) ($Ca+Mg$) vs. (HCO_3+SO_4), (d) ($Ca+Mg$) vs. HCO_3, (e) Ca vs. SO_4, (f) ($Ca+Mg$)-(HCO_3+SO_4) vs. [HCO_3+ SO_4].

Hydrol. Earth Syst. Sci. Discuss., https://doi.org/10.5194/hess-2017-647
Manuscript under review for journal Hydrol. Earth Syst. Sci.
Discussion started: 21 November 2017
© Author(s) 2017. CC BY 4.0 License.

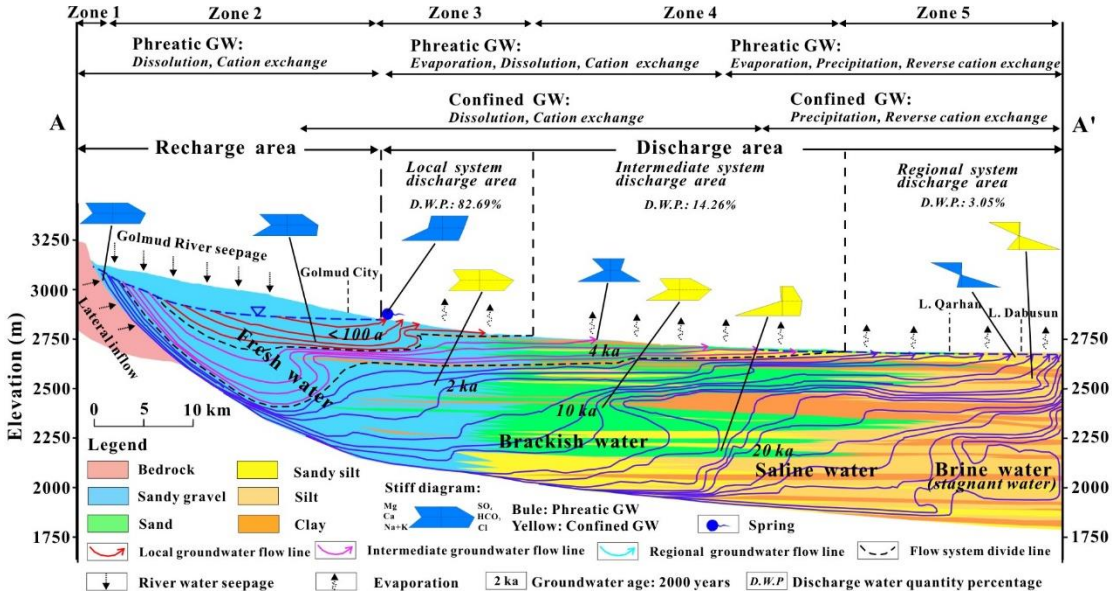

Figure 8: Conceptual model of groundwater flow and hydrochemical evolution in the Golmud watershed, China.

Hydrol. Earth Syst. Sci. Discuss., https://doi.org/10.5194/hess-2017-647
Manuscript under review for journal Hydrol. Earth Syst. Sci.
Discussion started: 21 November 2017
© Author(s) 2017. CC BY 4.0 License.

Hydrology and Earth System Sciences
Discussions

Table 1: Statistical summary of physical and chemical parameters of the surface water and groundwater in the Golmud Watershed, Qaidam Basin, China.

Place	Source		pH	TDS mg/L	Ca mg/L	Mg mg/L	Na mg/L	K mg/L	Cl mg/L	HCO_3 mg/L	SO_4 mg/L
Zone 2	RW	Min	8.03	393	30.9	26.3	63.0	3.7	87	184.0	68.5
		Max	8.41	523	38.9	36.4	92.1	5.3	144	214.6	100.5
		Average	8.28	462	35.8	32.1	80.2	4.5	114	198.1	85.4
	SGW	Min	7.62	236	14.8	18.9	78.5	2.0	90.33	89.09	28.82
		Max	8.83	1,171	86.2	80.0	232.2	10.7	436.7	309.0	235.0
		Average	8.07	618	49.0	36.4	131.0	6.9	173.7	221.8	116.0
Zone 3	RW	Min	8.25	368	37.7	24.4	56.1	3.5	77.4	178.1	68.7
		Max	8.55	1,266	64.2	83.9	276.0	13.3	382.0	335.0	256.0
		Average	8.43	670	49.1	42.8	139.8	6.8	177.5	232.8	133.9
	SGW	Min	7.42	443	20.6	16.9	98.0	2.0	83.1	132.0	116.2
		Max	9.32	12,116	359.0	474	3,385.0	187.0	4316	1018	3059
		Average	8.09	1853	81.9	81	476.9	22.7	554.9	293.0	501.9
	DGW	Min	7.89	404	30.0	18.6	65.9	4.1	84.0	204.8	41.4
		Max	8.64	676	52.4	37.7	162.0	9.7	145.0	310.0	218.0
		Average	8.19	547	41.3	29.9	95.3	6.2	93.7	248.2	88.3
Zone 4	RW	Min	7.94	616	39.7	38.7	104.5	5.5	152.0	246.0	97.5
		Max	8.64	1,833	82.6	116.9	432.2	18.7	580.7	448.0	382.3
		Average	8.29	1,013	55.9	57.7	232.7	9.6	289.3	303.1	191.1
	SGW	Min	7.08	528	10.4	15.5	102.0	5.2	83.1	48.4	97.9
		Max	9.34	185,006	2,048	4,058	56,200	1709	67,063	1179	82,202
		Average	8.01	32,029	322.7	635	10,464	248	11,550	375	8,627
	DGW	Min	7.83	514	6.7	8.0	68.7	4.0	84.0	39.9	63.9
		Max	8.69	7,184	456.0	48.6	2,048	39.8	1,292	445	3,648
		Average	8.25	1,401	59.0	24.8	406.8	8.4	263.1	269.3	483.2

Hydrol. Earth Syst. Sci. Discuss., https://doi.org/10.5194/hess-2017-647
Manuscript under review for journal Hydrol. Earth Syst. Sci.
Discussion started: 21 November 2017
© Author(s) 2017. CC BY 4.0 License.

Hydrology and Earth System Sciences
Discussions

Zone 5	RW	Min	8.73	1,741	56.1	92.8	437.9	12.1	655.2	159.7	208.1
		Max	9.45	3,268	81.0	118.5	996.3	18.9	1,776	448.3	396.8
		Average	9.09	2,319	70.7	106.3	628.3	15.3	1061	268.1	289.9
	FLW	Representative	8.98	10,937	113.7	696.3	2,957	231.8	5,912	314.9	660.7
	SLW	Min	6.03	399,098	116.2	99,500	4,137	3,168	276,849	1,941	7,717
		Max	6.28	403,758	177.2	100,240	4,740	4,122	285,780	3,118	10,894
		Average	6.16	401,428	146.7	99,870	4,439	3,645	281,315	2,530	9,306
	SGW	Min	6.03	336,229	1,541	53,480	12,388	11,798	215,561	506.0	984.5
		Max	8.56	361,200	5,871	64,860	35,712	22,351	239,340	874.3	8,313
		Average	7.30	348,715	3,706	59,170	24,050	17,075	227,451	690	4,649
	DGW	Representative	8.64	370,940	1,927	57,079	32,378	19,372	222,404		7,851

Table 2: Statistical summary of isotopic analysis results of precipitation, surface water and groundwater in the Golmud Watershed, Qaidam Basin, China.

Place	Source	δD ‰ VSMOW			$\delta^{18}O$ ‰ VSMOW			^{3}H TU			^{14}C pMC		
		Min	Max	Average	Min	Max	Average	Min	Max	Average	Min	Max	Average
Zone 1	Snowmelt			-77.0			-11.9						
	Precipitation	-85.3	-71.6	-75.2	-10.9	-9.3	-10.0						
	RW	-75.4	-64.8	-68.7	-11.1	-9.3	-10.1						
	GW			-65.0[a]			-9.7 [a]						
Zone 2	Precipitation	-68.1	-66.2	-67.2	-10.1	-9.7	-9.9						
	RW	-67.5	-63.2	-65.4	-10.7	-8.8	-9.6						
	SGW	-74.7	-58.0	-64.5	-10.9	-8.8	-9.8	20.0	56.3	35.5	30.6	57.9	42.5
Zone 3	RW	-70.8	-46.7	-63.6	-10.6	-4.8	-8.8						
	SGW	-74.8	-43.4	-63.5	-10.8	-4.3	-8.8	12.1	25.7	21.1	19.5	41.2	32.5

Hydrol. Earth Syst. Sci. Discuss., https://doi.org/10.5194/hess-2017-647
Manuscript under review for journal Hydrol. Earth Syst. Sci.
Discussion started: 21 November 2017
© Author(s) 2017. CC BY 4.0 License.

Hydrology and Earth System Sciences
Discussions

	DGW	-82.9	-52.1	-71.6	-11.2	-8.4	-10.3	＜1	10.1		0.7	49.15	23.4
Zone 4	RW	-67.7	-67.2	-67.5	-9.4	-7.1	-8.2						
	SGW	-75.6	-56.0	-68.0	-11.3	-7.1	-9.6	14.4	17.5	16.0	11.9	42.2	27.3
	DGW	-91.3	-51.4	-77.1	-12.8	-8.3	-11.2	＜1	4.1		1.9	38.6	14.8
Zone 5	RW			-51.3 [a]			-6.6 [a]						
	FLW			-20.0 [a]			0.6 [a]						
	SLW	-27.0	-4.0	-17.0	0.4	4.5	2.6						
	GW	-66.0	-2.0	-46.3	-10.8	-0.6	-8.2			18.9 [a,b]			

Note: a-Only one representative sample data; b-Shallow phreatic water sample data.

Table 3: Estimated parameters of different lithology from the Golmud Watershed, Qaidam Basin, China.

Lithology	K_h (m/d)	Anisotropy ratio K_h/K_v	Porosity
Gravel sand	56.3	10	0.35
Sand	13.7	10	0.40
Sandy silt	0.62	5	0.5
Silt	0.13	5	0.6
Clay	0.001	5	0.65